Two Dimensional DoA Using Non-Uniform L-Shaped Array

Yasoub Eghbali
Department of Electrical Engineering
Shahed University
Tehran, Iran
yasoubeghbali@gmail.com

Ali Panahzadeh
Department of Electrical Engineering
Shahed University
Tehran, Iran
ali.panahzadeh@chmail.ir

Mahmoud Ferdosizade Naeiny
Department of Electrical Engineering
Shahed University
Tehran, Iran
m.ferdosizade@shahed.ac.ir

***Abstract*—This study presents a new two dimensional (2-D) direction of arrival (DoA) estimation method. In the proposed method, an L-shaped array with non-uniform subarrays is used. By vectorizing of the covariance matrices of the subarrays along *x* and *z* axes, two new vectors are obtained. Using these vectors, two covariance matrices with Toeplitz structure are constructed. Applying the MUSIC algorithm to each Toeplitz covariance matrix, the azimuth and elevation angles of sources are estimated independently. To perform pair matching of the estimated angles, an extended vector can be obtained by concatenating the received signal vectors. By Eigen decomposition of the covariance matrix of the extended signal vector, the estimated azimuth and elevation angles are paired. Simulation results reveal that the proposed method improves the estimation accuracy of 2-D DoA estimation, and it can pair the azimuth and elevation angles with high probability of correct matching.**

Keywords—2-D DoA, Toeplitz, pair matching, L-shaped

I. INTRODUCTION

Two dimensional (2-D) DoA estimation is a fundamental problem in array signal processing, which has attracted attention in recent years due to its wide applications in various areas, including radar, sonar, source localization, communications, etc. [1]–[5]. Many geometrical arrays, such as L-shaped array [6], [7], circular array [8], [9], and rectangular array [10], [11] have been presented for 2-D DoA estimation.

Numerous algorithms, such as MUSIC [12], ESPRIT [13], and JSVD [14], have been proposed for DoA estimation, which can be applied to the received signal vector of an L-shaped array. Thus, the L-shaped array has attracted more attention in 2-D DoA estimation. The most existing methods for 2-D DoA estimation using an L-shaped array are based on the uniform linear subarrays. To increase the number of resolvable sources and to achieve high estimation accuracy, the number of antennas must be increased. Therefore, the computational complexity and hardware cost will be increased.

Nowadays, non-uniform linear arrays have attracted considerable attention due to the capability to reduce mutual coupling, enhancement of the estimation accuracy, and increasing the degree of freedom (DoF). The nested arrays [15] and the co-prime arrays [16] are two important classes of the non-uniform linear arrays. In [17], a 2-D DoA estimation method using an L-shaped array with two-level nested subarrays has been proposed. Using the cross-correlation matrix of the subarrays, the signal subspace is divided into two extended signal subspaces, and the azimuth and elevation angles are estimated independently. Also, a pair matching method for estimated azimuth and elevation angles has been presented, which are not suitable for the case that two or more sources have the same elevation or azimuth angles.

In this paper, a new 2-D DoA estimation method is presented. In the proposed method, two covariance matrices with Toeplitz structure are constructed using the received signal vector of the subarrays. Azimuth and elevation angles of the sources are estimated by applying the MUSIC algorithm to the obtained matrices. Then, a new vector is constructed by concatenating the received signal vector of two subarrays. Using the Eigen decomposition of the covariance matrix of this vector, the estimated azimuth and elevation angles are paired.

The paper is arranged as follows. In section II, the system model is introduced. The proposed 2-D DoA estimation method is described in section III. The proposed method for pair matching of the estimated azimuth and elevation angles is presented in section IV. In section V, simulation results are demonstrated. Finally, we conclude the paper in section VI.

II. SYSTEM MODEL

Consider an L-shaped array consists of two non-uniform linear subarrays on the *x* and *z* axes, as shown in Fig. 1. The antennas of the subarrays are located in the set of positions $\mathcal{S}_x = \{\alpha_1, \alpha_2, \dots, \alpha_{M_x}\}d_x$ and $\mathcal{S}_z = \{\beta_1, \beta_2, \dots, \beta_{M_z}\}d_z$. The spacing unit between antennas in both subarrays is equal to half-wavelength, i.e. $d_x = d_z = \lambda/2$.

Assume that the K narrowband signals are impinging on the array form the distinct directions. The direction of the k-th signal is (θ_k, ϕ_k), where θ_k denotes the azimuth angle and ϕ_k is the elevation angle. The received signal vector of the two subarrays can be represented as follows:

$$\mathbf{x}(t) = \mathbf{A}_x(\boldsymbol{\theta})\mathbf{s}(t) + \mathbf{n}_x(t) \tag{1}$$

$$\mathbf{z}(t) = \mathbf{A}_z(\boldsymbol{\phi})\mathbf{s}(t) + \mathbf{n}_z(t) \tag{2}$$

where $\mathbf{s}(t) = [s_1(t), s_2(t), \dots, s_K(t)]^T$ is the signal vector, $\mathbf{n}_x(t)$ and $\mathbf{n}_z(t)$ are the noise vectors of the *x* and *z* axes. Also, $\mathbf{A}_x(\boldsymbol{\theta})$ and $\mathbf{A}_z(\boldsymbol{\phi})$ are the steering matrices along *x* and *z* axes. The k-th column of $\mathbf{A}_x(\boldsymbol{\theta})$ and $\mathbf{A}_z(\boldsymbol{\phi})$ are defined as

$$\mathbf{a}_x(\theta_k) = \left[e^{j\pi\alpha_1 \cos\theta_k}, \dots, e^{j\pi\alpha_{M_x} \cos\theta_k}\right]^{\mathrm{T}} \tag{3}$$

978-1-7281-7296-5/20/$31.00 ©2020 IEEE

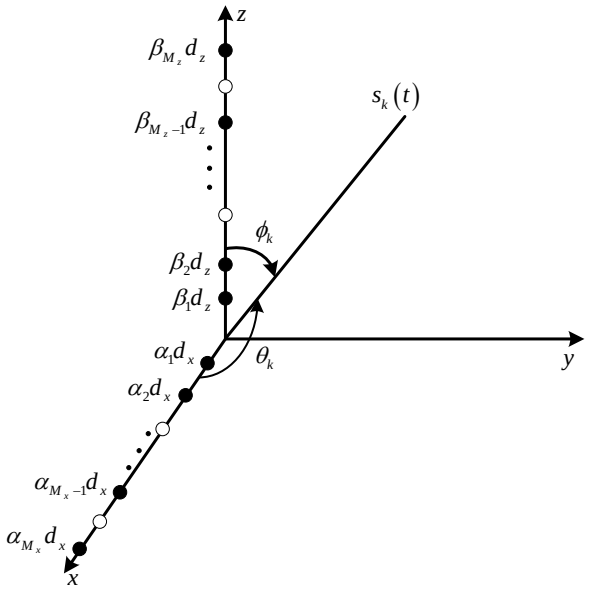

Fig. 1. L-shaped array with non-uniform linear subarrays.

$$\mathbf{a}_z(\phi_k) = \left[e^{j\pi\beta_1 \cos\phi_k}, \ldots, e^{j\pi\beta_{M_z}\cos\phi_k}\right]^{\mathrm{T}} \quad (4)$$

The covariance matrices of $\mathbf{x}(t)$ and $\mathbf{z}(t)$ can be represented as follows:

$$\mathbf{R}_x = E\{\mathbf{x}(t)\mathbf{x}^{\mathrm{H}}(t)\} = \mathbf{A}_x(\boldsymbol{\theta})\mathbf{R}_s\mathbf{A}_x^H(\boldsymbol{\theta}) + \sigma^2\mathbf{I}_{M_x} \quad (5)$$

$$\mathbf{R}_z = E\{\mathbf{z}(t)\mathbf{z}^{\mathrm{H}}(t)\} = \mathbf{A}_z(\boldsymbol{\phi})\mathbf{R}_s\mathbf{A}_z^H(\boldsymbol{\phi}) + \sigma^2\mathbf{I}_{M_z} \quad (6)$$

where $\mathbf{R}_s = E\{\mathbf{s}(t)\mathbf{s}^H(t)\}$ and σ^2 denotes the variance of noise. Also, $\mathbf{I}_{M_x}$ and $\mathbf{I}_{M_z}$ are identity matrices. In practice, the covariance matrices can be estimated using N snapshots of the received vectors as follows [18]:

$$\widehat{\mathbf{R}}_x = \frac{1}{N}\sum_{t=1}^{N}\mathbf{x}(t)\mathbf{x}^{\mathrm{H}}(t) \quad (7)$$

$$\widehat{\mathbf{R}}_z = \frac{1}{N}\sum_{t=1}^{N}\mathbf{z}(t)\mathbf{z}^{\mathrm{H}}(t) \quad (8)$$

III. Proposed 2-D DoA Estimation Method

In this section, a new 2-D DoA estimation method is presented. By vectorization of the covariance matrices of two subarrays, the following vectors can be obtained as follows:

$$\mathbf{y}_x = \mathrm{vec}(\mathbf{R}_x) = \mathbf{B}_x(\boldsymbol{\theta})\mathbf{p} + \sigma^2\mathrm{vec}(\mathbf{I}_{M_x}) \quad (9)$$

$$\mathbf{y}_z = \mathrm{vec}(\mathbf{R}_z) = \mathbf{B}_z(\boldsymbol{\phi})\mathbf{p} + \sigma^2\mathrm{vec}(\mathbf{I}_{M_z}) \quad (10)$$

where $\otimes$ stands for the kronecker product, $\mathbf{p} = [p_1, p_2, \ldots, p_K]^T$ is the signal power vector and

$$\mathbf{B}_x(\boldsymbol{\theta}) = [\mathbf{a}_x^*(\theta_1)\otimes\mathbf{a}_x(\theta_1), \ldots, \mathbf{a}_x^*(\theta_K)\otimes\mathbf{a}_x(\theta_K)] \quad (11)$$

$$\mathbf{B}_z(\boldsymbol{\phi}) = [\mathbf{a}_z^*(\phi_1)\otimes\mathbf{a}_z(\phi_1), \ldots, \mathbf{a}_x^*(\phi_K)\otimes\mathbf{a}_x(\phi_K)] \quad (12)$$

$\mathbf{y}_x$ and $\mathbf{y}_z$ are equivalent to the received signal vectors of two linear arrays with M_x^2 and M_z^2 antennas with the set of positions:

$$\mathcal{D}_x = \{(\alpha_m - \alpha_n)\frac{\lambda}{2}, 1 \le m, n \le M_x\} \quad (13)$$

$$\mathcal{D}_z = \{(\beta_m - \beta_m)\frac{\lambda}{2}, 1 \le m, n \le M_z\} \quad (14)$$

Considering the distinct elements of $\mathcal{D}_x$ and $\mathcal{D}_z$, two uniform linear arrays with the following measurement vectors will be obtained [19]:

$$\mathbf{r}_x \triangleq \mathbf{J}\mathbf{y}_x = \widetilde{\mathbf{A}}_x(\boldsymbol{\theta})\mathbf{p} + \sigma^2\mathbf{e}_x \quad (15)$$

$$\mathbf{r}_z \triangleq \mathbf{J}\mathbf{y}_z = \widetilde{\mathbf{A}}_z(\boldsymbol{\phi})\mathbf{p} + \sigma^2\mathbf{e}_z \quad (16)$$

where $\mathbf{J}_x$ and $\mathbf{J}_z$ are two selection matrices with the size of $(2\alpha_{M_x}+1)\times M_x^2$ and $(2\beta_{M_z}+1)\times M_z^2$, $\mathbf{e}_x$ and $\mathbf{e}_z$ are two vectors with the length of $2\alpha_{M_x}+1$ and $2\beta_{M_z}+1$, respectively. The k-th column of $\widetilde{\mathbf{A}}_x(\boldsymbol{\theta})$ and $\widetilde{\mathbf{A}}_z(\boldsymbol{\phi})$ are defined as:

$$\tilde{\mathbf{a}}_x(\theta_k) = \left[e^{-j\pi(\alpha_{M_x}-\alpha_1)\cos\theta_k}, \ldots, e^{j\pi(\alpha_{M_x}-\alpha_1)\cos\theta_k}\right]^T \quad (17)$$

$$\tilde{\mathbf{a}}_z(\phi_k) = \left[e^{-j\pi(\beta_{M_z}-\beta_1)\cos\phi_k}, \ldots, e^{j\pi(\beta_{M_z}-\beta_1)\cos\phi_k}\right]^T \quad (18)$$

The m-th element of $\mathbf{r}_x$ and $\mathbf{r}_z$ can be represented as follows:

$$r_x(m) = \sum_{k=1}^{K} p_k\, e^{j\pi m\cos\theta_k} + \sigma^2 e_{x,m},\ -\alpha_{M_x} \le m \le \alpha_{M_x} \quad (19)$$

$$r_z(m) = \sum_{k=1}^{K} p_k\, e^{j\pi m\cos\phi_k} + \sigma^2 e_{z,m},\ -\beta_{M_z} \le m \le \beta_{M_z} \quad (20)$$

where $e_{x,m}$ and $e_{z,m}$ are defined as:

$$e_{x,m} = \begin{cases} 1, & m = 0 \\ 0, & m \ne 0 \end{cases} \quad (21)$$

$$e_{z,m} = \begin{cases} 1, & m = 0 \\ 0, & m \ne 0 \end{cases} \quad (22)$$

Based on (19) and (20), the following relationship can be obtained [20]:

$$r_{xt}(m,n) \triangleq E\{r_x(m)r_x^*(n)\} =$$
$$\left(\sum_{k=1}^{K} p_k e^{-j\pi m\cos\theta_k} + \sigma^2 e_{x,m}\right)\left(\sum_{l=1}^{K} p_l e^{-j\pi n\cos\theta_l} + \sigma^2 e_{x,n}\right)^* = \sum_{l=1}^{K} p_l e^{j\pi n\cos\theta_l}\left(\sum_{k=1}^{K} p_k e^{-j\pi m\cos\theta_k} + \sigma^2 e_{x,m}\right) + \sigma^2 e_{x,n}\sum_{k=1}^{K} p_k e^{-j\pi m\cos\theta_k} + \sigma^4 e_{x,m}e_{x,n} \quad (23)$$

$$r_{zt}(m,n) \triangleq E\{r_z(m)r_z^*(n)\}$$

$$= \left(\sum_{k=1}^{K} p_k e^{-j\pi m cos\phi_k} + \sigma^2 e_{z,m}\right)\left(\sum_{l=1}^{K} p_l e^{-j\pi n cos\phi_l} + \sigma^2 e_{z,n}\right)^* = \sum_{l=1}^{K} p_l e^{j\pi n cos\phi_l}\left(\sum_{k=1}^{K} p_k e^{-j\pi m cos\phi_k} + \sigma^2 e_{z,m}\right) + \sigma^2 e_{z,n}\sum_{k=1}^{K} p_k e^{-j\pi m cos\phi_k} + \sigma^4 e_{z,m}e_{z,n} \quad (24)$$

The following relations are defined:

$$cx_{m,l} \triangleq p_l\left(\sum_{k=1}^{K} p_k e^{-j\pi m cos\theta_k} + \sigma^2 e_{x,m}\right) \quad (25)$$

$$cz_{m,l} \triangleq p_l\left(\sum_{k=1}^{K} p_k e^{-j\pi m cos\phi_k} + \sigma^2 e_{z,m}\right) \quad (26)$$

$$gx_{m,n} \triangleq \sigma^2 e_{x,m}\sum_{k=1}^{K} p_k e^{-j\pi m cos\theta_k} \quad (27)$$

$$gz_{m,n} \triangleq \sigma^2 e_{z,m}\sum_{k=1}^{K} p_k e^{-j\pi m cos\phi_k} \quad (28)$$

Using the above definition, (23) and (24) can be rewritten as:

$$r_{xt}(m,n) \triangleq \sum_{k=1}^{K} cx_{m,l} e^{j\pi n cos\theta_k} + cx_{m,l} + \sigma^4 e_{x,m}e_{x,m} \quad (29)$$

$$r_{zt}(m,n) \triangleq \sum_{k=1}^{K} cz_{m,l} e^{j\pi n cos\phi_k} + cz_{m,l} + \sigma^4 e_{z,m}e_{z,m} \quad (30)$$

Two Toeplitz covariance matrices can be constructed as (31) and (32), which are shown in the bottom of the page. In (31) and (32), h_{xm}, h_{zm}, $\mathbf{I}_{\alpha_{M_x}+1,m}$ and can be defined:

$$h_{xm} = \sigma^2 \sum_{k=1}^{K} p_k e^{-j\pi m cos\theta_k} \quad (33)$$

$$h_{zm} = \sigma^2 \sum_{k=1}^{K} p_k e^{-j\pi m cos\phi_k} \quad (34)$$

$$\mathbf{I}_{\alpha_{M_x}+1,m} = \begin{cases} \mathbf{I}_{\alpha_{M_x}+1}, & m = 0 \\ \mathbf{0}_{\alpha_{M_x}+1}, & m \neq 0 \end{cases} \quad (35)$$

$$\mathbf{I}_{\beta_{M_z}+1,m} = \begin{cases} \mathbf{I}_{\beta_{M_z}+1}, & m = 0 \\ \mathbf{0}_{\beta_{M_z}+1}, & m \neq 0 \end{cases} \quad (36)$$

and

$$\mathbf{A}_{xt} = [\mathbf{a}_{xt}(\theta_1), \mathbf{a}_{xt}(\theta_2), \ldots, \mathbf{a}_{xt}(\theta_K)] \quad (37)$$

$$\mathbf{A}_{zt} = [\mathbf{a}_{zt}(\phi_1), \mathbf{a}_{zt}(\phi_2), \ldots, \mathbf{a}_{zt}(\phi)] \quad (38)$$

The k-th column of $\mathbf{A}_{xt}$ and $\mathbf{A}_{zt}$ can be represented as

$$\mathbf{a}_{xt}(\theta_k) = \left[1, e^{-j\pi cos\theta_k}, \ldots, e^{-j\pi\alpha_{M_x} cos\theta_k}\right]^T \quad (39)$$

$$\mathbf{a}_{zt}(\phi_k) = \left[1, e^{-j\pi cos\phi_k}, \ldots, e^{-j\pi\beta_{M_z} cos\phi_k}\right]^T \quad (40)$$

$\mathbf{A}_{xt}$ and $\mathbf{A}_{zt}$ have the Vandermonde structure; therefore, $\mathbf{R}_{xt}(m)$, and $\mathbf{R}_{zt}(m)$ are full-rank. The Eigen decomposition of the Toeplitz matrices can be expressed as follows:

$$\mathbf{R}_{xt}(m) = \mathbf{U}_{xs}\mathbf{\Lambda}_{xs}\mathbf{U}_{xs}^H + \mathbf{U}_{xn}\mathbf{\Lambda}_{xn}\mathbf{U}_{xn}^H \quad (41)$$

$$\mathbf{R}_{zt}(m) = \mathbf{U}_{zs}\mathbf{\Lambda}_{zs}\mathbf{U}_{zs}^H + \mathbf{U}_{zn}\mathbf{\Lambda}_{zn}\mathbf{U}_{zn}^H \quad (42)$$

where $\mathbf{U}_{xs}$ and $\mathbf{U}_{zs}$ denote the signal subspace eigenvectors, $\mathbf{U}_{xn}$ and $\mathbf{U}_{zn}$ are the noise subspace eigenvectors, $\mathbf{\Lambda}_{xs}$ and $\mathbf{\Lambda}_{zs}$ are the signal eigenvalues, $\mathbf{\Lambda}_{xn}$ and $\mathbf{\Lambda}_{zn}$ stand for the noise eigenvalues. Since in equation (31), $\mathbf{A}_{xt}$ only depends on the azimuth angles of the sources and in equation (32), $\mathbf{A}_{zt}$ depends on only the elevation angles of the sources, then using the MUSIC algorithm, the azimuth and elevation angles of sources can be estimated independently.

IV. Pair Matching

The main challenge after the separate estimation of the azimuth and elevation angles is pair matching. It means that we don't know which elevation and azimuth angles belong to the same source. In this section, a new approach is presented for pair matching of the estimated angles. By concatenating the vectors of two subarrays, a new vector can be obtained as follows:

$$\mathbf{y}(t) = \begin{bmatrix}\mathbf{x}(t)\\ \mathbf{z}(t)\end{bmatrix} = \mathbf{A}(\boldsymbol{\theta}, \boldsymbol{\phi})\mathbf{s}(t) + \begin{bmatrix}\mathbf{n}_x(t)\\ \mathbf{n}_z(t)\end{bmatrix} \quad (43)$$

where $\mathbf{A}(\boldsymbol{\theta}, \boldsymbol{\phi}) = [\mathbf{A}_x^T(\boldsymbol{\theta})\ \mathbf{A}_z^T(\boldsymbol{\phi})]^T$. The covariance matrix of $\mathbf{y}(t)$ can be represented as follows:

$$\mathbf{R}_{\mathrm{y}} = \mathbf{A}(\boldsymbol{\theta}, \boldsymbol{\phi})\mathbf{R}_{\mathrm{s}}\mathbf{A}^{\mathrm{H}}(\boldsymbol{\theta}, \boldsymbol{\phi}) + \sigma^2\mathbf{I}_{\mathrm{M}_x+\mathrm{M}_z} \quad (44)$$

Eigen decomposition of $\mathbf{R}_{\mathrm{y}}$ is described below:

$$\mathbf{R}_{\mathbf{y}} = \mathbf{U}_{\mathrm{y_s}}\mathbf{\Lambda}_{\mathrm{y_s}}\mathbf{U}_{\mathrm{y_s}}^{\mathrm{H}} + \sigma^2\mathbf{U}_{\mathrm{y_s}}\mathbf{U}_{\mathrm{y_s}}^{\mathrm{H}} \quad (45)$$

$$\mathbf{R}_{xt} = \begin{bmatrix} r_{xt}(m,0) & r_{xt}(m,1) & \cdots & r_{xt}(m,\alpha_{M_x}) \\ r_{xt}(m,-1) & \vdots & \ddots & r_{xt}(m,\alpha_{M_x}+1) \\ \vdots & \ddots & \vdots & \vdots \\ r_{xt}(m,-\alpha_{M_x}) & r_{xt}(m,-\alpha_{M_x}+1) & \cdots & r_{xt}(m,0) \end{bmatrix} = \mathbf{A}_{xt}\mathrm{diag}(cx_{m,1}, \ldots, cx_{m,K})\mathbf{A}_{xt}^H + h_{xm}\mathbf{I}_{\alpha_{M_x}+1,m} + \sigma^4\mathbf{I}_{\alpha_{M_x}+1,m} \quad (31)$$

$$\mathbf{R}_{zt} = \begin{bmatrix} r_{zt}(m,0) & r_{zt}(m,1) & \cdots & r_{zt}(m,\beta_{M_z}) \\ r_{zt}(m,-1) & \vdots & \ddots & r_{zt}(m,\beta_{M_z}+1) \\ \vdots & \ddots & \vdots & \vdots \\ r_{zt}(m,-\beta_{M_x}) & r_{zt}(m,-\beta_{M_z}+1) & \cdots & r_{zt}(m,0) \end{bmatrix} = \mathbf{A}_{zt}\mathrm{diag}(cz_{m,1}, \ldots, cz_{m,K})\mathbf{A}_{zt}^H + h_{xm}\mathbf{I}_{\beta_{M_z}+1,m} + \sigma^4\mathbf{I}_{\beta_{M_z}+1,m} \quad (32)$$

In the proposed method, it is assumed that the elevation and azimuth angles are estimated independently using a 1-D MUSIC algorithm. In practice, the azimuth or elevation angles of two or more sources may be the same. In this case, the number of estimated azimuth angles or the number of estimated elevation angles are lower than the number of sources. Suppose that $\hat{\boldsymbol{\theta}} = \{\hat{\theta}_1, \hat{\theta}_2, \dots, \hat{\theta}_{K_1}\}$ and $\hat{\boldsymbol{\phi}} = \{\hat{\phi}_1, \hat{\phi}_2, \dots, \hat{\phi}_{K_2}\}$ are the sets of the estimated angles. The k-th signal angles can be paired by solving the following optimization problem:

$$\{\hat{\theta}_k, \hat{\phi}_k\} = \underset{i\in\{1,\dots,K_1\}, j\in\{1,\dots,K_2\}}{\operatorname{argmin}} \left\|\mathbf{a}(\hat{\theta}_i, \hat{\phi}_j)\mathbf{U}_{\mathrm{s}}\right\|_2^2 \tag{46}$$

The details of the proposed method are summarized in Algorithm 1. It is noteworthy that unlike the method in [17], the proposed method can perform well when some of the sources have the same elevation or azimuth angles.

Algorithm 1 Summary of the proposed method

Input: $\mathbf{x}(t), \mathbf{z}(t), t = 1, 2, \dots, N$ and number of sources K.

Output: $\{\hat{\theta}_k, \hat{\varphi}_k\}_{k=1}^{K}$

a. Estimate $\hat{\mathbf{R}}_x$ and $\hat{\mathbf{R}}_z$ using (7) and (8).

b. Compute $\mathbf{y}_x$ and $\mathbf{y}_z$ using (9) and (10).

c. Compute $\mathbf{r}_x$ and $\mathbf{r}_z$ using (15) and (16).

d. Construct the matrices $\mathbf{R}_{xt}(m)$ and $\mathbf{R}_{zt}(m)$ using (31) and (32).

e. Estimate the azimuth and elevation angles by applying the MUSIC algorithm on $\mathbf{R}_{xt}(m)$ and $\mathbf{R}_{zt}(m)$.

$k = 1$

while $(k \le K)$ **do**

Pair the angles using (46).

$k = k + 1$

end while

V. Simulation Results

In this section, simulation results are presented to evaluate the performance of the proposed method. Root mean square error (RMSE) is used as a metric to evaluate the accuracy of the proposed method. RMSE of 2-D DoA estimation is defined as follows:

$$\text{RMSE} = \sqrt{\frac{1}{2KL}\sum_{l=1}^{L}\sum_{k=1}^{K}\left(\theta_k - \hat{\theta}_{k,l}\right)^2 + \left(\phi_k - \hat{\phi}_{k,l}\right)^2} \tag{47}$$

where L is the number of Monte-Carlo iterations, $\hat{\theta}_{k,l}$ and $\hat{\phi}_{k,l}$ are the estimates of θ_k and ϕ_k in the l-th Monte-Carlo iteration. The number of Monte-Carlo iterations is considered to be $L = 10^3$.

In [17], a subspace extension method using an L-shaped array with two-level nested subarrays has been proposed. The angles are estimated using the cross-correlation matrix of the subarrays. It is worth noting that the proposed pair matching method in [17] is not suitable for the case that two or more sources have the same elevation or azimuth angles. The performance of the proposed method is compared with the proposed method in [17].

In our proposed method, an L-shaped array with augmented nested arrays (ANA) is considered [20]. Also, for the subspace extension method, a two-level nested array is deployed. It is worth noting that the number of antennas of all subarrays is identical $(M = M_x = M_z = 10)$. The antenna locations of non-uniform subarrays are given in Table I.

In the first set of simulations, $K = 2$ uncorrelated signals with angles $\boldsymbol{\theta} = [10, 60]^\circ$ and $\boldsymbol{\phi} = [20, 50]^\circ$ are considered. In Fig. 2, the Cramer-Rao bound (CRB) of the L-shaped arrays with different geometries is depicted. As shown in Table I, the ANA geometry has more DoF; therefore, the CRB with ANA geometry is lower than the CRB with two-level nested array geometry.

In Fig. 3, the performance of the proposed method is compared with the method in [17] at N = 400. As can be seen from this figure, the proposed method has a lower RMSE.

In Fig. 4, the RMSE of the proposed is compared with the method in [17] at SNR = 0dB when a different number of snapshots are used. As can be seen from this figure, the proposed method has a lower RMSE than the subspace extension method.

In Fig. 5, the probability of correct pair matching of the proposed method is compared with the proposed method in [17]. In the low SNR, the proposed method has a higher probability of correct pair matching than the subspace extension method.

TABLE I. The Location of the Physical Antennas for Non-Nuiform Arrays

Array Geometry	The Set of Positions	DoF
Two-Level Nested Array	{1, 2, 3, 4, 5, 6, 10, 14, 18, 22}	43
ANA	{1, 2, 4, 6, 12, 18, 24, 30, 31, 33}	53

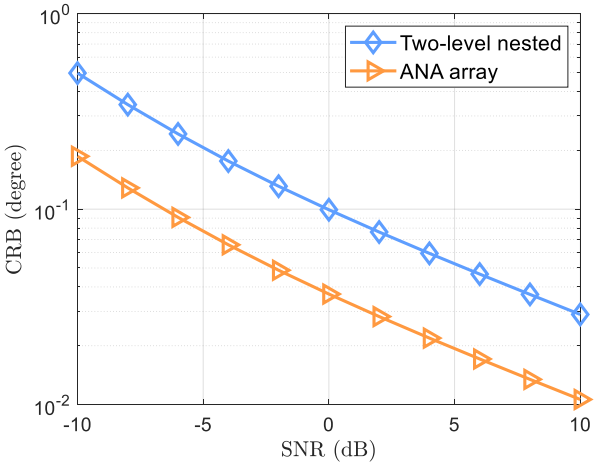

Fig. 2. CRB versus SNR for $K = 2$ sources with $\boldsymbol{\theta} = [10, 60]^\circ$, $\boldsymbol{\phi} = [20, 50]^\circ$, and $N = 400$.

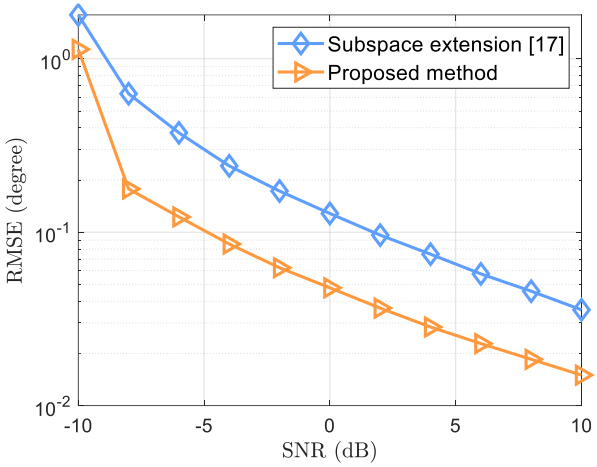

Fig. 3. RMSE versus SNR for $K = 2$ sources with $\boldsymbol{\theta} = [10, 60]°$, $\boldsymbol{\phi} = [20, 50]°$, and $N = 400$.

In the last simulations, three sources are considered, in which the first and second sources have the same elevation angles. In Fig. 6, the probability of correct pair matching of our method is depicted. The proposed pair matching method can pair the angles in the case that there are sources with the same azimuth or elevation angles.

VI. Conclusion

In this paper, a new 2-D DoA estimation method using an L-shaped array with non-uniform subarrays was proposed. By vectorization of the covariance matrices of the subarrays, two new vectors were obtained. Using these vectors, two covariance matrices with Toeplitz structure were constructed. Applying the MUSIC algorithm to the Toeplitz matrices, the azimuth and elevation angles were estimated independently. Also, a new pair matching method was presented. Simulation results reveal that the proposed method has achieved a better performance than the conventional subspace extension algorithm.

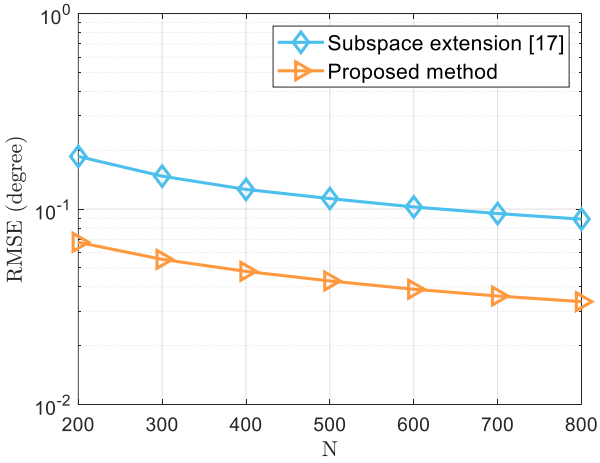

Fig. 4. RMSE versus the number of snapshots, N, for $K = 2$ sources with $\boldsymbol{\theta} = [10, 60]°$, $\boldsymbol{\phi} = [20, 50]°$, and SNR = 0dB.

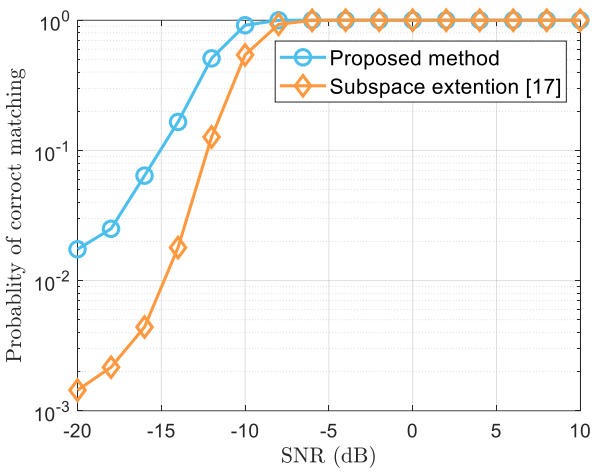

Fig. 5. Probability of correct pair matching versus SNR for $K = 2$ sources with $\boldsymbol{\theta} = [10, 60]°$, $\boldsymbol{\phi} = [20, 50]°$, and $N = 200$.

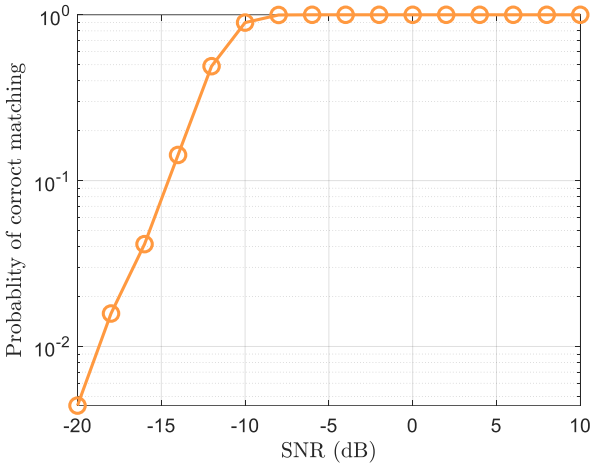

Fig. 6. Probability of correct pair matching versus SNR for $K = 3$ sources with $\boldsymbol{\theta} = [10, 40, 60]°$, $\boldsymbol{\phi} = [20, 20, 50]°$, and $N = 200$.

References

[1] Y. Dong, C. Dong, W. Liu, H. Chen and G. Zhao, "2-D DoA Estimation for L-Shaped Array with Array Aperture and Snapshots Extension Techniques," *IEEE Signal Processing Letters*, vol. 24, no. 4, pp. 495-499, 2017.

[2] J. Jia-jia, D. Fa-jie and W. Xian-Quan, "A Universal Two-Dimensional Direction of Arrival Estimation Method Without Parameter Match," *IEEE Sensors Journal*, vol. 16, no. 9, pp. 3141-3146, 2016.

[3] Y. Dong, C. Dong, Z. Shen and G. Zhao, "Conjugate Augmented Spatial Temporal Technique for 2-D DoA Estimation with L-Shaped Array," *IEEE Antennas and Wireless Propagation Letters*, vol. 14, pp. 1622-1625, 2015.

[4] N. Tayem, K. Majeed and A. A. Hussain, "Two-Dimensional DoA Estimation Using Cross-Correlation Matrix with L-Shaped Array," *IEEE Antennas and Wireless Propagation Letters*, vol. 15, pp. 1077-1080, 2016.

[5] F. Shi, "Two Dimensional Direction-of-Arrival Estimation Using Compressive Measurements," *IEEE Access*, vol. 7, pp. 20863-20868, 2019.

[6] N. Xi and L. Liping, "A Computationally Efficient Subspace Algorithm for 2-D DoA Estimation with L-Shaped Array," *IEEE Signal Processing Letter*, vol. 21, no. 8, pp. 971–974, 2014.

[7] J. F. Gu, W. P. Zhu, and M. N. S. Swamy, "Joint 2-D DoA Estimation via Sparse L-Shaped Array," *IEEE Transaction on Signal Processing*, vol. 63, no. 5, pp. 1171–1182, 2015.

[8] B. H. Wang, H. T. Hui, and M. S. Leong, "Decoupled 2-D Direction of Arrival Estimation Using Compact Uniform Circular Arrays in the Presence of Elevation-Dependent Mutual Coupling," *IEEE Transaction on Antennas Propagation*, vol. 58, no. 3, pp. 747–755, 2010.

[9] B. R. Jackson, S. Rajan, B. J. Liao, and S. Wang, "Direction of arrival estimation using directive antennas in uniform circular arrays," IEEE Trans. on Antennas Propag., vol. 63, no. 2, pp. 736–747, 2015.

[10] Z. Ye and C. Liu, "2-d doa estimation in the presence of mutual coupling," *IEEE Transaction on Antennas Propagation*, vol. 56, no. 10, pp. 3150–3158, 2008.

[11] P. Heidenreich, A. M. Zoubir, and M. Rubsamen, "Joint 2-d doa estimation and phase calibration for uniform rectangular arrays," *IEEE Transaction on Signal Processing*, vol. 60, no. 9, pp. 4683–4693, 2012.

[12] R. O. Schmidt, "Multiple emitter location and signal parameter estimation," *IEEE Transactions on Antennas and Propagation*, vol. 34, no. 3, pp. 276–280, 1986.

[13] R. Roy and T. Kailath, "ESPRIT-estimation of signal parameters viarotational invariance techniques," *IEEE Transaction on Acoustic, Speech, Signal Processing*, vol. 37, no. 7, pp. 984-995, 1989.

[14] J. Gu and P. Wei, "Joint SVD of Two Cross-Correlation Matrices to Achieve Automatic Pairing in 2-D Angle Estimation Problems," *IEEE Antennas and Wireless Propagation Letters*, vol. 6, pp. 553-556, 2007.

[15] P. Pal and P. P. Vaidyanathan, "Nested Arrays: A Novel Approach to Array Processing with Enhanced Degrees of Freedom," *IEEE Transaction on Signal Processing*, vol. 58, no. 8, pp. 4167–4181, 2010.

[16] P. P. Vaidyanathan and P. Pal, "Sparse Sensing with Co-Prime Samplers and Arrays," *IEEE Transaction on Signal Processing*, vol. 59, no. 2, pp. 573–586, 2011.

[17] S. Liu, L. Yang, D. Li and H. Cao, "Subspace Extension Algorithm for 2D DOA Estimation with L-shaped Sparse Array," *Multidimensional Systems and Signal Processing*, vol. 6, no. 1, pp. 315-327, 2017.

[18] Y. Eghbali and M. F. Naeiny, "Off-grid DoA Estimation Method of Wideband Signals," *Intenational Journal of Communication Systems*, vol. 33 , no. 14, pp. 1-14, 2020.

[19] Y. Eghbali and M. F. Naeiny, "DFT Based Direction of Arrival Estimation Using Minimum Nested Array," *IET Signal Processing*, vol. 14 , no. 2, pp. 47-55, 2019.

[20] J. Liu, Y. Zhang, Y. Lu, S. Ren and S. Cao, "Augmented Nested Arrays With Enhanced DOF and Reduced Mutual Coupling," *IEEE Transactions on Signal Processing*, vol. 65, no. 21, pp. 5549-5563, 2017.